J. Biochem. 2021;170(3):317–326 doi:10.1093/jb/mvab044

JB THE JOURNAL OF BIOCHEMISTRY

# Bisecting-GlcNAc on Asn388 is characteristic to ERC/mesothelin expressed on epithelioid mesothelioma cells

*Received November 27, 2020; accepted March 27, 2021; published online April 1, 2021*

**Haruhiko Fujihira[1,2,*], Daisuke Takakura[3,4], Atsushi Matsuda [5], Masaaki Abe[6], Michiyo Miyazaki[3], Tomomi Nakagawa[3], Kazunori Kajino[6,7], Kaori Denda-Nagai[1], Miki Noji[1], Okio Hino[6] and Tatsuro Irimura [1,†]**

[1]Division of Glycobiologics, Intractable Disease Research Center, Juntendo University Graduate School of Medicine, 2-1-1 Hongo Bunkyo-ku, Tokyo 113-8421, Japan; [2]Glycometabolic Biochemistry Laboratory, Cluster for Pioneering Research, RIKEN, 2-1 Hirosawa, Wako, Saitama 351-0198, Japan; [3]Project for Utilizing Glycans in the Development of Innovative Drug Discovery Technologies, Japan Bioindustry Association (JBA), 2-26-9 Hatchobori, Cho-ku, Tokyo 104-0032, Japan; [4]Graduate School of Medical Life Science, Yokohama City University, 1-7-29 Suehiro, Tsurumi, Yokohama, Kanagawa 230-0045, Japan; [5]Department of Biochemistry, School of Medicine, Keio University, 35 Shinanomachi, Shinjuku-ku, Tokyo 160-8582, Japan; [6]Department of Pathology and Oncology, Juntendo University Faculty of Medicine, 2-1-1 Hongo, Bunkyo-ku, Tokyo 113-8421, Japan; and [7]Department of Human Pathology, Juntendo University Faculty of Medicine, 2-1-1 Hongo, Bunkyo-ku, Tokyo 113-8421, Japan

*Haruhiko Fujihira, Division of Glycobiologics, Intractable Disease Research Center, Juntendo University Graduate School of Medicine, Tokyo 113-8421, Japan. Tel: +81-3-3830-8715, Fax: +81-3-3830-8715, email: h-fujihira@juntendo.ac.jp

[†]Tatsuro Irimura, Division of Glycobiologics, Intractable Disease Research Center, Juntendo University Graduate School of Medicine, Tokyo 113-8421, Japan. Tel: +81-3-5802-1876, Fax: +81-3-3830-8715, email: t-irimura@juntendo.ac.jp

**Mesothelioma is a highly aggressive tumour associated with asbestos exposure and is histologically classified into three types: epithelioid-type, sarcomatoid-type and biphasic-type. The prognosis of mesothelioma patients is poor and there is no effective molecular-targeting therapy as yet. ERC/mesothelin is a glycoprotein that is highly expressed on several types of cancers including epithelioid mesothelioma, but also expressed on normal mesothelial cells. This is a predicted reason why there is no clinically approved therapeutic antibody targeting ERC/mesothelin. In the present study, we focussed on the differential glycosylation between ERC/mesothelin present on epithelioid mesothelioma and that on normal mesothelial cells and aimed to reveal a distinct feature of epithelioid mesothelioma cells. Lectin microarray analysis of ERC/mesothelin using cells and patient specimens showed significantly stronger binding of PHA-$E_4$ lectin, which recognizes complex-type *N*-glycans having a so-called bisecting-GlcNAc structure, to ERC/mesothelin from epithelioid mesothelioma cells than that from normal mesothelial cells. Further, liquid chromatography/mass spectrometry**

## Graphical Abstract

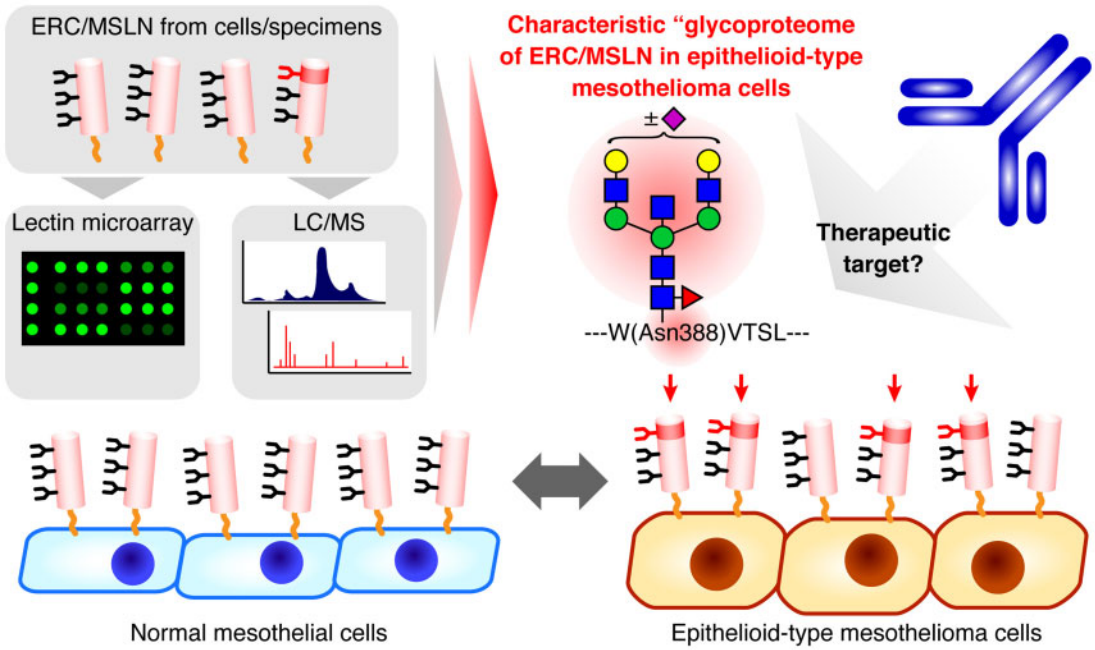

**analysis on ERC/mesothelin from epithelioid mesothelioma cells confirmed the presence of a bisecting-GlcNAc attached to Asn388 of ERC/mesothelin. These results suggest that this glycoproteome could serve as a potential target for the generation of a highly selective and safe therapeutic antibody for epithelioid mesothelioma.**

*Keywords:* bisecting-GlcNAc; epithelioid mesothelioma; ERC/mesothelin; glycosylation.

*Abbreviations:* ACN, acetonitrile; ERC/MSLN, ERC/mesothelin; FBS, foetal bovine serum; GPI, glycosylphosphatidylinositol; LC/MS, liquid chromatography/mass spectrometry; PAGE, polyacrylamide gel electrophoresis; SDS, sodium dodecyl sulphate

Mesothelioma is an aggressive tumour originating from pleura, peritoneum or pericardial cavity, and is usually caused by exposure to asbestos (*1–3*). The incubation period of asbestos-related mesothelioma is estimated to be ~30–40 years. In Japan, the incidence of mesothelioma patients has been increasing and is predicted to reach a peak in 2030 (*4*). In most developed countries, the use of asbestos has been prohibited, but in developing countries it is still used (*3*). Therefore, the number of mesothelioma cases is predicted to increase in the future worldwide. Mesothelioma is histologically classified into three types: epithelioid-type, sarcomatoid-type and biphasic-type, and the prognosis of mesothelioma patients is poor regardless of the type (*5*). Therefore, the development of an effective therapy including molecular-targeting therapies against mesothelioma is urgently needed, while it has not been achieved yet.

ERC/mesothelin (ERC/MSLN; ERC is a name from "expressed in renal carcinoma") is a glycosylphosphatidylinositol (GPI)-anchored cell surface glycoprotein highly expressed in epithelioid mesothelioma, pancreatic cancer and ovarian cancer (Fig. 1A) (*6*). ERC/MSLN is synthesized as a ~71 kDa precursor form and is later cleaved into two products (a 40 kDa C-terminal product and a 31 kDa N-terminal product) by furin-like protease. The C-terminal product, which is anchored on the cell surface, is called ERC/MSLN (*6*). The N-terminal product, which is secreted into the blood, is reported to be a good serum biomarker for mesothelioma diagnosis (*7*). ERC/MSLN has been a potential drug target molecule for several cancers; however, there is no clinically applied therapy targeting ERC/MSLN. One reason is the wide expression of ERC/MSLN on normal mesothelial cells that might cause adverse effects.

Glycosylation is one of the major co- and post-translational modifications of proteins (*8*). It is well known that cellular glycosylation drastically changes upon malignant transformation of mammalian cells (*9*). Also, protein glycosylation is known to be involved in the malignant behaviours of cancer cells (*10–13*), which are often acquired during cancer progression. Alterations in the glycosylation of cancer cells result from various intrinsic factors affecting glycosylation, including differential expression of glycosyltransferases and enzymes responsible for the supply of precursor molecules. The changes include altered regulation at the transcriptional level (*14–17*), alterations of chaperon functions (*18*, *19*) and altered glycosidases (*20*). However, little is known about the differential glycosylation of ERC/MSLN and other cell surface molecules expressed by mesothelioma. Attempts to utilize such differential glycosylation in the diagnosis and therapy of mesothelioma have not been previously made.

In the present study, we aimed to reveal a characteristic glycoform of ERC/MSLN on epithelioid mesothelioma. The characteristic 'glycoproteome (= glycoform + peptide sequence)' of ERC/MSLN on epithelioid mesothelioma cells may be useful to overcome adverse effects in the therapeutic use of anti-ERC/MSLN antibodies against epithelioid mesothelioma. To this end, we performed comprehensive glycan analysis using lectin microarray. A characteristic glycan structure and its attachment site distinctive to epithelioid mesothelioma cells were further confirmed by liquid chromatography/mass spectrometry (LC/MS). The identified structure may represent a characteristic glycoproteome of ERC/MSLN on epithelioid mesothelioma: bisecting-GlcNAc containing glycans on Asn388 of ERC/MSLN. This glycoproteome could be the key for the development of specific therapeutic antibodies for epithelioid mesothelioma. Our results shed some light on the development of a therapy for several types of cancers focussing on differential glycosylation of a molecule expressed on both normal and cancer cells.

## Materials and Methods

### *Ethics statement*

This study was approved by the Institutional Review Board of Juntendo University Graduate School of Medicine (#201713). Patient specimens (tissue sections) were obtained from archived paraffin-embedded tumour blocks from biopsies or surgeries.

### *Cell culture*

Epithelioid mesothelioma cell lines (H226 [NCI-H226], MESO-4 [ACC-MESO4]), immortalized non-tumorous mesothelial cell line (MeT-5A), and primary normal mesothelial cells (MES-F) were cultivated in RPMI1640 (Gibco) [supplemented with 10% foetal bovine serum (FBS), 10 mM HEPES], Medium 199 (Sigma) (supplemented with 10% FBS, 3.3 nM epidermal growth factor, 400 nM hydrocortisone, 870 nM zinc-free bovine insulin, 20 mM HEPES, trace elements), Medium 199 (Sigma) (supplemented with 10% FBS, penicillin streptomycin), respectively, at 37°C in a 5% $CO_2$ atmosphere.

### *Preparation of cell lysates*

Cultured cells were washed with phosphate buffered saline (PBS) 3 times and collected using a cell scraper. Fifty million cells were suspended with 1 ml of PBS containing 0.5% Nonidet P40 (NP-40) (FUJIFILM Wako), homogenized using a syringe and needle (gauge: 21G) on ice, and incubated on ice for at least 10 min. The samples were centrifuged at 10,000×*g* for 10 min at 4°C and the obtained supernatants were used as cell lysate. The protein concentration of the prepared cell lysates was measured by BCA protein assay (Pierce) with bovine serum albumin as a standard.

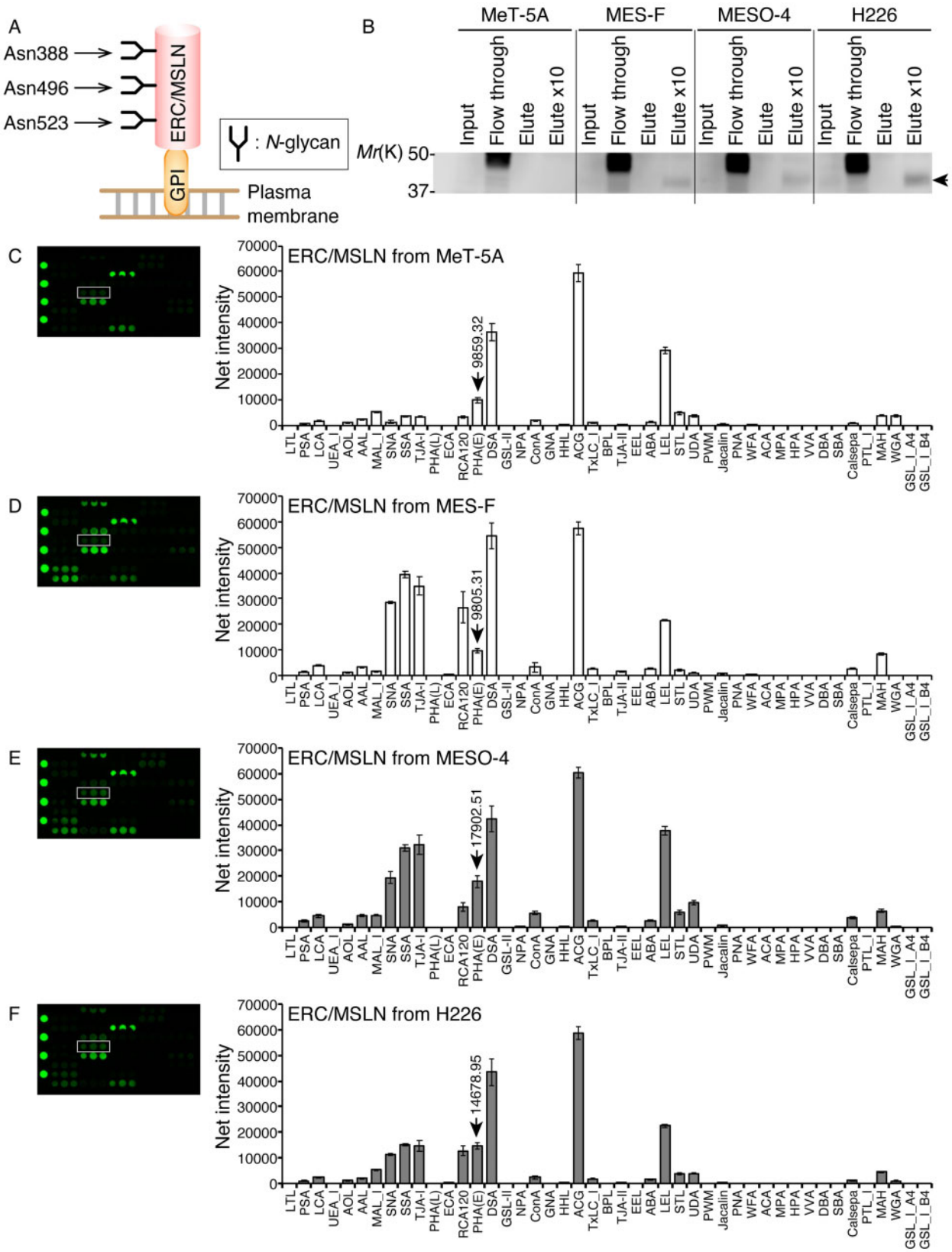


**Fig. 1. PHA-E4 lectin strongly binds to ERC/MSLN from epithelioid mesothelioma cells compared to that from normal mesothelial cells.** (**A**) Schematic representation of ERC/MSLN. Asn388, Asn496 and Asn523 indicate glycosylation sites. (**B**) Western blotting to confirm the immunoprecipitation of ERC/MSLN from cell lines. Arrow indicates ERC/MSLN. Elute x 10: 10 times amount of elutes were loaded. (**C–F**) Scan images and bar graphs of glycan profiling analysis of ERC/MSLN from MeT-5A (C), MES-F (D), MESO-4 (E) and H226 cells (F) using lectin microarray ($n = 3$). White squares in scan images and arrows in bar graphs indicate the position of PHA-$E_4$ lectin. The numbers above the arrows indicate the net intensity of PHA-$E_4$ lectin. Error bar indicates standard deviation.

### *Protein extraction from patient specimens*

Formalin-fixed, paraffin-embedded tissue sections from 4 epithelioid mesothelioma patients were used. The tissue sections were deparaffinized, and the parts containing epithelioid mesothelioma were scratched from the glass slide using a needle (gauge size: 29G) under the microscope. The scratched tissue fragments were collected into a 1.5 ml microtube containing 400 µl of 10 mM citrate buffer (pH 6.0) and incubated at 95°C for 60 min for antigen retrieval. After cooling on ice, 10–20 µl of 50% (v/v) Avicel PH-105 (DuPont, coprecipitating reagent) in PBS was added and mixed. The mixture was centrifuged at 5,000×*g* for 3 min, and the supernatant was removed. After washing with PBS by centrifugation, the tissue pellets were solubilized with 50–100 µl of PBS containing 1% (w/v) NP-40 and sonicated gently. The tissue suspension was incubated on ice for 60 min and then centrifuged at 10,000×*g* for 2 min at 4°C. The obtained supernatants were used as tissue lysates.

### *Immunoprecipitation and lectin precipitation*

Immunoprecipitation was performed as described previously (*21*). Briefly, 200 µg of prepared cell lysates and 50 µl of tissue lysates (corresponding to about 8 $mm^2$) were subjected to immunoprecipitation using biotinylated-mouse-anti-ERC/MSLN antibody (IBL, clone 22A31, #10357). The cell/tissue lysates were shaken with a 200 µl slurry of Dynabeads My One Streptavidin T1 (Dyna-SA) (Veritas, #DB65604) at 4°C for at least 60 min for preclearing. Two hundred and fifty nanograms of biotinylated-anti-ERC/MSLN antibody was immobilized to a 200 µl slurry of Dyna-SA by shaking at 4°C for at least 60 min. Biotinylated-anti-ERC/MSLN antibody immobilized Dyna-SA (bio-anti-ERC/MSLN-beads) was washed with TBS containing 1% (w/v) Triton-X 100 (TBSTx) 3 times. Precleared lysates and washed bio-anti-ERC/MSLN-beads were mixed and shaken at 4°C for 16 h. The supernatant was removed, and the beads were washed with TBSTx 3 times. Washed beads were suspended into 10 µl of TBS containing 0.2% (w/v) sodium dodecyl sulphate (SDS) and incubated at 95°C for 10 min to elute the precipitated ERC/MSLN. Incubated samples were centrifuged at 10,000×*g* for 2 min, and the supernatants were collected. Collected supernatants were shaken with a 20 µl slurry of Dyna-SA at 4°C for at least 60 min to deplete the eluted biotinylated antibody. The samples were centrifuged at 10,000×*g* for 1 min at 4°C, and the supernatants were collected and used as IP-ERC/MSLN. For lectin precipitation, 25 µl of IP-ERC/MSLN from cells (corresponding to 50 µg of cell lysates) was used. IP-ERC/MSLN was mixed with 2 µg of biotinyated-PHA-$E_4$ lectin and a 10 µl slurry of Dyna-SA and shaken at 4°C for 16 h. After washing with TBSTx 3 times, the beads were suspended into 20 µl of TBS containing 0.2% (w/v) SDS and incubated at 95°C for 10 min to elute the precipitated ERC/MSLN. Eluted ERC/MSLN was shaken with a 20 µl slurry of Dyna-SA to deplete eluted biotinylated-PHA-$E_4$ lectin. The depleted samples were centrifuged at 10,000×*g* for 1 min at 4°C, and the obtained supernatants were used as PHA-$E_4$ precipitated ERC/MSLN.

### *Antibody-overlay lectin microarray analysis*

Antibody-overlay lectin microarray was performed as described previously (*22*) to obtain the glycan profile of IP-ERC/MSLN. Briefly, 10 µl of IP-ERC/MSLN was diluted with Probing solution (GlycoTechnica), applied to the LecChip (GlycoTechnica) and incubated at 20°C for 16 h. After the incubation, 20 µg of human IgG (FUJIFILM Wako) was added to each well and incubated at 20°C for 30 min (*22*). After washing with PBS containing 1% (w/v) Triton-X 100 (PBSTx) 3 times, 60 µl of Probing solution containing 20 µg of human IgG and 200 ng of biotinylated-mouse-anti-ERC/MSLN antibody (clone 22A31, described under Immunoprecipitation and lectin precipitation section) was added to each well and incubated at 20°C for 1 h. After washing with PBSTx 3 times, 60 µl of Probing solution containing 400 ng of Cy3-streptavidin (GE Healthcare) was added to each well and incubated at 20°C for 30 min. After washing with PBSTx 3 times, 60 µl of Probing solution was added to each well and scanned using GlycoStation Reader 1200 (GlycoTechnica). All data were analysed with Signal Capture 1.5 (GlycoTechnica) and GlycoStation ToolsPro 1.5 (GlycocTechnica). The net intensity of each spot was calculated by subtracting the background value from the total signal intensity of three spots.

### *Western blotting*

Samples (cell lysates, immunoprecipitation flow through, IP-ERC/MSLN) were separated by SDS–polyacrylamide gel electrophoresis (PAGE) and electroblotted onto polyvinylidene fluoride (PVDF) membranes. The membrane was blocked for 60 min with 4% Block Ace (KAC Co., Ltd. Kyoto, Japan) at 37°C, and incubated with primary antibody (2.5 µg/ml) in antibody diluting reagent (KIWAMI SETSUYAKUKUN, DRC, Co., Ltd, Tokyo, Japan) at 37°C for 1 h, followed by secondary antibody in antibody diluting reagent at 37°C for 1 h. The chemiluminescence was analysed with C-DiGit membrane scanner (LI-COR, Lincoln, NE, USA) using ImmunoStar LD (FUJIFILM Wako).

### *In-gel digestion*

An improved in-gel digestion method was used as described in a previous study (*23*). IP-ERC/MSLN was prepared from membrane proteins of H226 cells. SDS–PAGE was performed using 5–20% precast gradient gels (DRC, Tokyo, Japan) under a constant current of 21 mA for 90 min. The proteins were visualized by Pierce Silver Stain for Mass Spectrometry (Thermo), and the protein bands corresponding to IP-ERC/MSLN were excised. The washed gel pieces were incubated with 100 µl of reduction buffer containing 10 mM DTT in 25 mM ammonium bicarbonate (pH 8.0) in the presence of 0.2 M guanidinium chloride (GuHCl) at 56°C for 1 h. The gel pieces were subsequently alkylated with an equal volume of 55 mM iodoacetamide at room temperature for 30 min in the dark. After washing with 25 mM ammonium bicarbonate (pH 8.0)/50% acetonitrile (ACN) for 2 h (with a buffer change every 15 min) to remove the excess salt, 20 µl (2 ng/µl) of trypsin solution (Promega) with 0.01% trypsin enhancer were added to the gel pieces and incubated on ice for 10 min. Then, 15 µl of 0.01% trypsin enhancer in 25 mM ammonium bicarbonate (pH 8.0) were added and incubated at 37°C for 3 h. Tryptic digests were extracted in a stepwise manner with 20 µl of 10%, 20%, 30%, 40% and 50% ACN by shaking and sonication for 10 and 5 min, respectively. All the extracts were combined and dried using a speed-vac concentrator. A portion of the extracted glycopeptides was deglycosylated using the IGOT method (*24*). The remaining glycopeptides were enriched with a 5-fold volume of cold acetone by centrifugation at 12,000×*g* for 10 min (*25*).

### *LC/MS*

Deglycosylated peptides and glycopeptides were separated on an LC20AD system (SHIMADZU) with MonoCap C18 trap column (0.2 mm × 50 mm, GL Science) and a Nano HPLC Capillary Column (75 µm × 120 mm, 3 µm, C18; Nikkyo Technos). The eluents consisted of water containing 0.1% (v/v) formic acid (pump A) and ACN containing 0.1% (v/v) formic acid (pump B). The glycopeptides were eluted at a flow rate of 0.3 µl/min with a linear gradient from 2% to 35% B over 40 min. Mass spectra were acquired on a Q Exactive mass spectrometer (Thermo Fisher Scientific) equipped with Nanospray Flex Ion Source (Thermo Fisher Scientific) operated in the positive ion mode. Full mass spectra were acquired by using an $m/z$ range of 350–2,000 for deglycosylated peptides or 700–2,000 for glycosylated peptides with a resolution of 70,000. Product ion mass spectra were acquired against the 10 most intense ions by using a data-dependent acquiring method with a resolution of 17,500 with normalized collision energy of 27%. Deglycosylated peptides were identified by the SEQUEST search engine using UniprotKB database (status/2017/12). The following parameters were applied to the search: a specified trypsin enzymatic cleavage with two possible missed cleavages, a precursor mass tolerance of 6 ppm, a fragment mass tolerance of 0.02 Da, static modification of cysteine (carbamidomethylation), and dynamic modifications of methionine (oxidation), asparagine [delta: H(−1)N(−1)18O(*1*)], and N-term glutamine (Gln > PyroGlu).

### *Site-specific glycosylation analysis*

Product ion spectra of glycopeptides were manually selected based on the identification of oligosaccharide oxonium ions, with a characteristic $m/z$ such as 366.14 (HexNAc-Hex). The peptide and glycan masses of glycopeptides were deduced from the molecular masses of the peptide ion carrying a single HexNAc. Monosaccharide glycoform compositions were deduced using GlycoMod tool software. The remaining glycoforms were found from mass intervals between the glycoforms, and their peak areas

were calculated from the extracted ion chromatograms and summed across all charge states of glycoforms.

#### Statistical analysis

Statistical analysis was performed using R software. Wilcoxon rank sum test was used to evaluate differences in relative fluorescence intensities of PHA-$E_4$/ACG or RCA120/ACG among normal mesothelial cells, epithelioid mesothelioma cells and epithelioid mesothelioma patient specimens.

## Results

### PHA-$E_4$ lectin binds more strongly to ERC/MSLN derived from epithelioid mesothelioma cells than to that from normal mesothelial cells

To reveal a structural characteristic of ERC/MSLN on epithelioid mesothelioma cells, ERC/MSLN was immunoprecipitated from cell lysates of normal mesothelial primary culture cells (MES-F), an immortalized nontumorous mesothelial cell line (MeT-5A), and two epithelioid mesothelioma cell lines (H226 and MESO-4). Immunoprecipitation of ERC/MSLN was confirmed by western blotting (Fig. 1B). Equal amounts of immunoprecipitated-ERC/MSLN (IP-ERC/MSLN), calibrated based on western blotting band intensities, were subjected to lectin microarray analysis. As a result, we found that PHA-$E_4$ lectin showed a higher reactivity against IP-ERC/MSLN from epithelioid mesothelioma cell lines than that from normal mesothelial cells (Fig. 1C–F). On the other hand, RCA120 lectin showed a lower reactivity against IP-ERC/MSLN from epithelioid mesothelioma cell lines compared to that from normal mesothelial primary culture cells (Fig. 1D–F). Other lectins did not show any differential reactivity against IP-ERC/MSLN between epithelioid mesothelioma and normal mesothelial cells. A glycan structure that increases in epithelioid mesothelioma cells could be a distinct feature of epithelioid mesothelioma, therefore, we focussed on PHA-$E_4$ lectin binding.

### The strong binding of PHA-$E_4$ lectin to epithelioid mesothelioma derived ERC/MSLN is further validated using epithelioid mesothelioma patient specimens

To validate the PHA-$E_4$ lectin binding to epithelioid mesothelioma derived ERC/MSLN, we performed lectin precipitation. Equal amounts of IP-ERC/MSLN, calibrated based on western blotting band intensities (Fig. 2A, lower panel), were subjected to PHA-$E_4$ lectin precipitation. PHA-$E_4$ lectin precipitated a greater portion of IP-ERC/MSLN from epithelioid mesothelioma cell lines (H226 and MESO-4) than from normal mesothelial primary culture cells (MES-F) (Fig. 2A, upper panel). PHA-$E_4$ lectin is known to bind to complex-type *N*-glycans with a bisecting-GlcNAc residue (*26*). To investigate if the PHA-$E_4$ binding to IP-ERC/MSLN from epithelioid mesothelioma cells is *N*-glycan-dependent, we treated IP-ERC/MSLN from H226 cells with PNGase F and conducted lectin microarray analysis. Upon PNGase F treatment, almost all lectin signals including PHA-$E_4$ disappeared (Fig. 2B), confirming that PHA-$E_4$ lectin binding depends on *N*-glycans present on ERC/MSLN. Next, we performed lectin microarray analysis using ERC/MSLN derived from epithelioid mesothelioma patient specimens. Epithelioid mesothelioma cells were obtained from surgical specimens, and ERC/MSLN was immunoprecipitated from prepared tissue extracts. IP-ERC/MSLN from the tissues were subjected to lectin microarray analysis. Our analysis revealed that PHA-$E_4$ binding was also high in ERC/MSLN derived from surgical specimens (Fig. 2C). Because ACG lectin showed consistently high intensities among all lectins when ERC/MSLN was subjected to lectin array analysis, we compared the relative binding intensities of PHA-$E_4$ versus ACG among normal mesothelial cells, mesothelioma cells and mesothelioma specimens (Fig. 2D). As a result, PHA-$E_4$ showed a significantly stronger binding to IP-ERC/MSLN from epithelioid mesothelioma cells than to that from normal mesothelial cells.

### Structural determinations of N-glycans from ERC/MSLN of epithelioid mesothelioma cells

We performed LC/MS analysis of IP-ERC/MSLN from an epithelioid mesothelioma cell line (H226) to confirm the presence of glycans that are recognized by PHA-$E_4$ lectin, *i.e.* 'bisecting-GlcNAc'. ERC/MSLN was isolated from H226 cells by immunoprecipitation followed by separation on SDS–PAGE (Fig. 3A). The protein was subjected to in-gel tryptic digestion. A portion of in-gel digested samples was analysed by the isotope-coded glycosylation site-specific tagging (IGOT) method (Fig. 3B) (*24*). The rest of in-gel digested samples was directly analysed by LC/MS (Fig. 3B) after glycopeptide enrichment. ERC/MSLN has three potential *N*-glycosylation sites (Asn388, Asn496 and Asn523) and all of these glycosylation sites were glycosylated according to the results of our analysis (Fig. 3C–E and Table I). When we estimated the glycan structures at each site from the $m/z$ and MS/MS analyses (Supplementary Fig. S2A–C), glycans were highly heterogeneous. The glycans estimated to contain bisecting-GlcNAc residues were most abundant at Asn388, accounting for 11% of total *N*-glycans attached to this site (Fig. 3C). Glycans estimated to contain bisecting-GlcNAc were also observed at Asn496, but the relative content was very low (2.7% of total *N*-glycans attached to this site) (Fig. 3D). Glycans attached to Asn523 did not contain bisecting-GlcNAc (Fig. 3E). Our lectin microarray and LC/MS analyses indicate that ERC/MSLN from H226 cells carries glycans containing a bisecting-GlcNAc residue mainly at the Asn388 position.

## Discussion

In the present study, we comparatively analysed glycoforms of ERC/MSLN derived from epithelioid mesothelioma cells versus those derived from normal mesothelial cells to identify a characteristic structure in epithelioid mesothelioma cells. Results of our lectin microarray analysis revealed that PHA-$E_4$ lectin showed significantly stronger binding to ERC/MSLN from epithelioid mesothelioma cells than that from normal mesothelial cells. Similarly, ERC/MSLN from

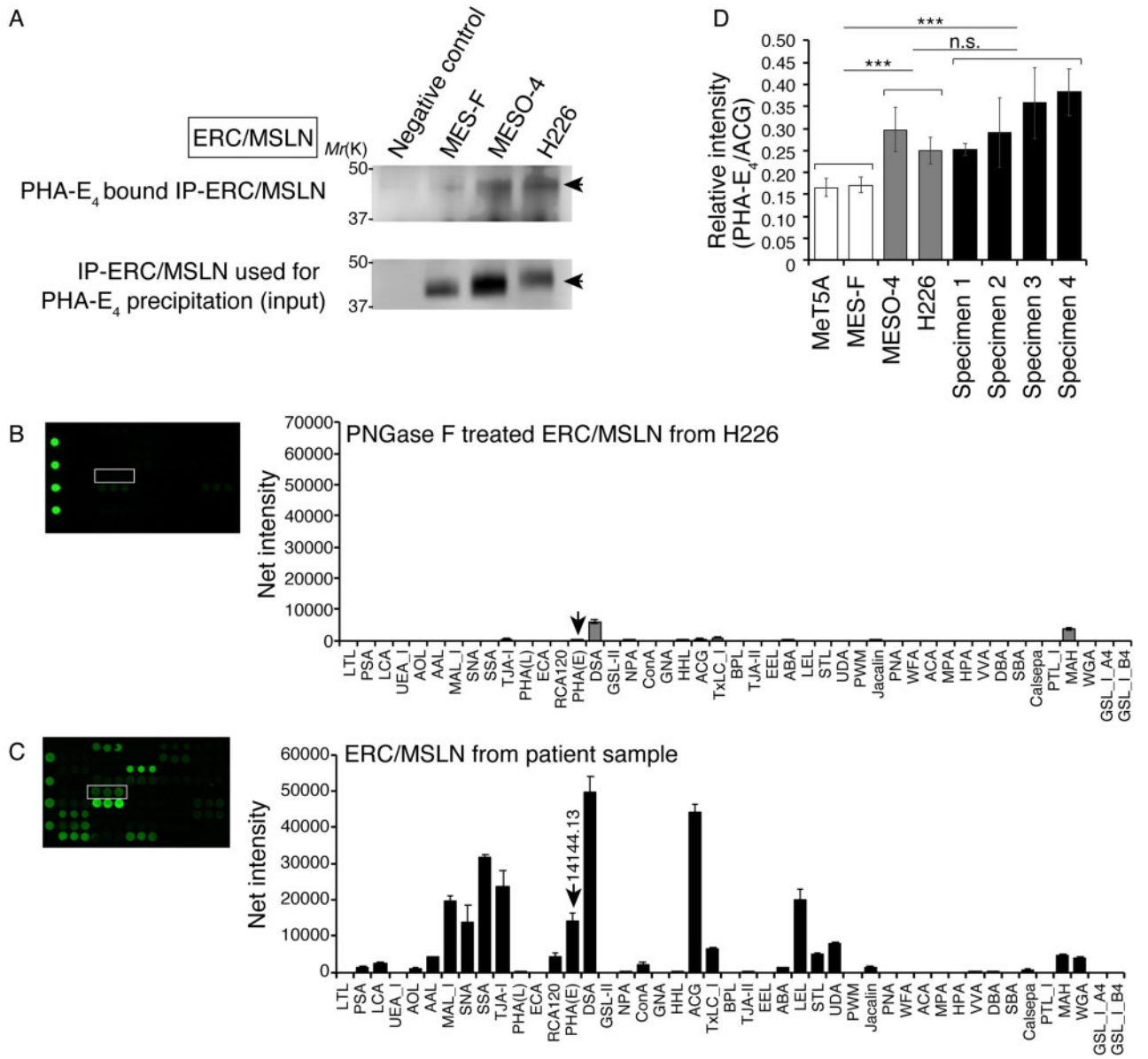


**Fig. 2. PHA-E4 lectin binds to N-glycans on ERC/MSLN from epithelioid mesothelioma cell lines and to ERC/MSLN from epithelioid mesothelioma patient specimens to a similar extent.** (**A**) Western blotting using anti-ERC/MSLN antibody to validate PHA-$E_4$ binding against ERC/MSLN. Lower panel shows the amount of IP-ERC/MSLN used for lectin (PHA-$E_4$) precipitation (input). Upper panel shows the amount of precipitated IP-ERC/MSLN. Arrow indicates ERC/MSLN. (**B**) Scan image and bar graph of glycan profiling of PNGase F-treated ERC/MSLN from H226 cells. (**C**) Scan image and bar graph of glycan profiling of ERC/MSLN from patient specimens ($n = 3$). A representative data among four patient specimens is shown (C). White squares in scan images and arrows in bar graphs indicate the position of PHA-$E_4$ lectin. The numbers above the arrows indicate the net intensity of PHA-$E_4$ lectin. Error bar: standard deviation. (**D**) Comparison of relative PHA-$E_4$ binding intensity among cell lines (MeT-5A, MES-F, MESO-4, H226) and patient specimens (patients 1–4). Error bar indicates standard deviation. Wilcoxon rank sum test was used for statistical analysis. $^{***}P < 0.005$, n.s., not significant.

surgical specimens from mesothelioma patients also showed significantly stronger reactivity with PHA-$E_4$ lectin. On the other hand, both ERC/MSLN from epithelioid mesothelioma cells and surgical specimens showed a significantly weaker reactivity with RCA120 lectin than that from normal mesothelial primary culture cells (Supplementary Fig. S1C). Therefore, the characteristic glycoforms of ERC/MSLN from epithelioid mesothelioma cells are clinically relevant. The structural feature of ERC/MSLN, having bisecting-GlcNAc recognized by PHA-$E_4$ lectin, could be used as a target to develop specific therapies or as a biomarker for epithelioid mesothelioma.

PHA-$E_4$ lectin is known to bind to complex-type *N*-glycans having bisecting-GlcNAc residues (*27*). On the other hand, RCA120 lectin is known to bind to complex-type *N*-glycans having terminal galactose residues (*28*). The insertion of bisecting-GlcNAc is thought to inhibit *N*-glycan branching (*29–32*) and might reduce terminal galactose residues. This could explain why PHA-$E_4$ lectin binding was increased and RCA120 lectin binding was decreased in epithelioid

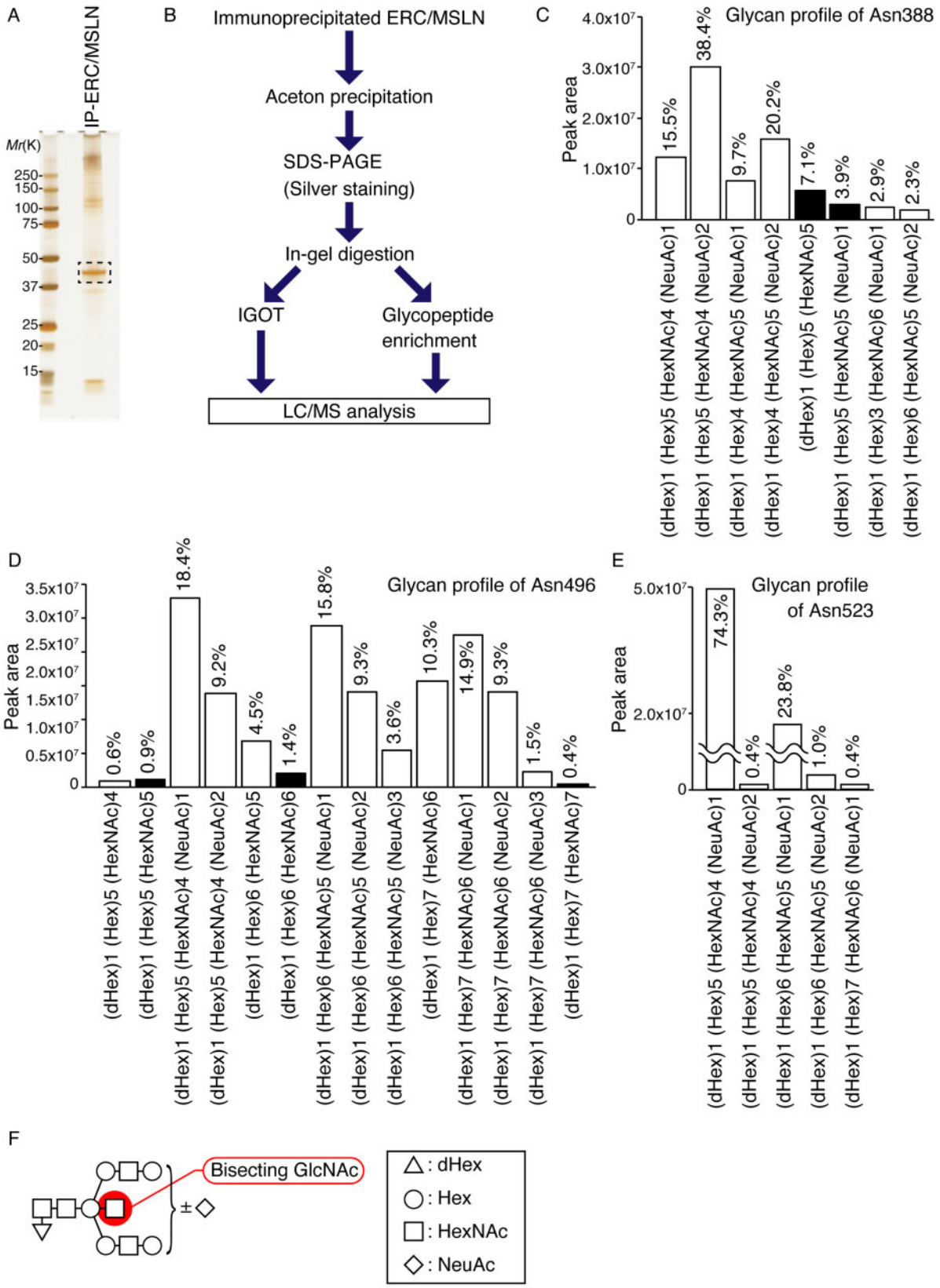


**Fig. 3. Bisecting-GlcNAc, the glycan structure recognized by PHA-E4, predominantly exists on the Asn388 residue of ERC/MSLN derived from epithelioid mesothelioma cells.** (**A**) Silver staining result of IP-ERC/MSLN from H226 cells. Dotted line square indicates ERC/MSLN and digested position used for LC/MS analysis. (**B**) Flow chart showing the sample preparation of ERC/MSLN from H226 cells for glycan analysis by LC/MS. (**C–E**) Glycan profile of ERC/MSLN at Asn388 (C), Asn496 (D) and Asn523 (E). Black bar indicates glycan structures containing bisecting-GlcNAc, and white bar indicates glycan structures without bisecting-GlcNAc. (**F**) Expected glycan structure containing bisecting-GlcNAc. dHex, deoxyhexose; Hex, hexose; HexNAc, *N*-acetylhexosamine; NeuAc, *N*-acetylneuraminic acid.

**Table I Glycopeptide sequences of ERC/MSLN from H226 cells identified by LC/MS analysis**

| Glycosite | Sequence | MW |
|---|---|---|
| Asn388 | (K) W**N**VTSLETLK (A) | 1189.63 |
| | (R) KW**N**VTSLETLK (A) | 1317.73 |
| | (K) W**N**VTSLETLKALLEVNK (G) | 1957.09 |
| | (R) KW**N**VTSLETLKALLEVNK (G) | 2085.18 |
| | (K) MSPEDIRKW**N**VTSLETLK (A) | 2146.11 |
| | (K) M*SPEDIRKW**N**VTSLETLK (A) | 2162.10 |
| | (K) W**N**VTSLETLKALLEVNKGHEMSPQVATLIDR (F) | 3491.84 |
| | (K) W**N**VTSLETLKALLEVNKGHEM*SPQVATLIDR (F) | 3507.84 |
| Asn496 | (R) LAFQNM**N**GSEYFVK (I) | 1646.78 |
| | (R) LAFQNM*NGSEYFVK (I) | 1662.78 |
| | (K) ARLAFQN/M**N**GSEYFVK (I) | 1873.91 |
| | (K) ARLAFQNM*NGSEYFVK (I) | 1889.91 |
| | (R) LAFQNM**N**GSEYFVKIQSFLGGAPTEDLK (A) | 3103.53 |
| | (R) LAFQNM*NGSEYFVKIQSFLGGAPTEDLK (A) | 3119.53 |
| Asn523 | (K) ALSQQ**N**VSMDLATFMK (L) | 1782.86 |
| | (K) ALSQQ**N**VSM*DLATFMK (L) | 1798.86 |
| | (K) ALSQQ**N**VSMDLATFMKLR(T) | 1814.85 |
| | (K) ALSQQ**N**VSMDLATFMKLR(T) | 2052.05 |
| | (K) ALSQQ**N**VSM*DLATFMKLR(T) | 2068.04 |
| | (K) ALSQQ**N**VSM*DLATFM*KLR (T) | 2084.04 |
| | (K) IQSFLGGAPTEDLKALSQQ**N**VSMDLATFMK (L) | 3239.62 |
| | (K) IQSFLGGAPTEDLKALSQQ**N**VSM*DLATFMK (L) | 3255.61 |
| | (K) IQSFLGGAPTEDLKALSQQ**N**VSM*DLATFM*K (L) | 3271.61 |

M*: methionine oxidation, **N**: glycosylation site.

mesothelioma cell-derived ERC/MSLN. In the present study, lectin microarray and LC/MS corroborate each other to show that *N*-glycans of ERC/MSLN synthesized by mesothelioma cells contain a bisecting-GlcNAc residue. Mass to charge signals derived from bisecting-GlcNAc structures were most abundant in *N*-glycans attached to Asn388, while none was present in *N*-glycans attached to Asn523. These results suggest that the glycopeptide which includes Asn388 and bisecting-GlcNAc could serve as a characteristic 'glycoproteome' to epithelioid mesothelioma cells. Molecular mechanisms regulating the extension and the peripheral modification of each glycan on a glycoprotein are not fully understood. Coordinated events during the transport of glycoproteins through intracellular compartments, particularly various portions of the endoplasmic reticulum and Golgi apparatus, should be carefully considered. We speculate that Asn388 of ERC/MSLN forms a structure which MGAT3 can preferentially access compared to two other *N*-glycosylation sites. Further studies are needed to clarify the detailed molecular mechanism by which the formation of bisecting-GlcNAc mainly occurs at Asn388 of ERC/MSLN.

Formation of bisecting-GlcNAc residues in *N*-glycans is catalyzed by *N*-acetylglucosaminyltransferase III (GnT-III) (*26*). GnT-III or its product, bisecting-GlcNAc, were reported to be upregulated in some cancer cells, while their contribution to cancer growth and aggressiveness differs depending on cancer types (*33–36*). Interestingly, an upregulation of bisecting-GlcNAc was observed in cancer cells expressing high levels of ERC/MSLN, such as ovarian endometrioid carcinoma cells and pancreatic ductal carcinoma cells (*33*, *34*). Therefore, it is likely that ERC/MSLN with *N*-glycans containing bisecting-GlcNAc may contribute to the malignant behaviour of epithelial mesothelioma, ovarian endometrioid carcinoma, and pancreatic ductal carcinoma. In line with this thought, we confirmed that the *GnT-III* (*MGAT3*) expression level is significantly higher in epithelioid mesothelioma cells (H226, MESO-4) than in normal mesothelial cells (MeT-5A) (Supplementary Fig. S3A). A role for *N*-glycans with bisecting-GlcNAc in modulating the expression and functions of some glycoproteins, such as E-cadherin, was previously reported (*37–42*). E-cadherin is a transmembrane glycoprotein involved in cell-cell adhesion (*43*), and bisecting-GlcNAc modification of its *N*-glycans altered its membrane expression (*44*). ERC/MSLN was also reported to be involved in cell adhesion (*45*), but the roles of its *N*-glycans and their glycoforms remain to be clarified. Our preliminary results of cell proliferation assay using *MGAT3*-KO MESO-4 cells, which we generated using the CRISPR/Cas9 system, showed a reduced cell proliferation rate in *MGAT3*-KO cells (Supplementary Fig. S3D). We confirmed that PHA-$E_4$ reactivity was reduced concomitant with a decrease in *MGAT3* expression levels in *MGAT3*-KO cells (Supplementary Fig. S2B and C). Therefore, MGAT3 seems to contribute, at least in part, to the proliferation of epithelioid mesothelioma cells.

In summary, our study provides a characteristic glycoproteome of ERC/MSLN expressed on epithelioid mesothelioma cells, with ERC/MSLN having complex-type *N*-glycans containing a bisecting-GlcNAc predominantly on Asn388. A specific antibody generated against this glycoproteome could be an effective therapy for epithelioid mesothelioma and would potentially show less adverse effects than currently available therapeutic antibodies. In addition, having glycans containing a bisecting-GlcNAc residue may be a prerequisite for ERC/MSLN to be involved in the malignant

behaviour of certain cancers cells with high expression levels of ERC/MSLN.

## Supplementary Data

Supplementary Data are available at *JB* Online.

## Acknowledgements

We wish to thank the members of the Division of Glycobiologics for fruitful discussion. We also thank Dr. Katrin Beate Ishii-Schrade for her valuable comments on this manuscript.

### Funding

This work was supported by the Japan Agency for Medical Research and Development (JP19ae0101026) and in part by the Japan Society for the Promotion of Science Grants-in-Aid for Scientific Research (18K14655 to H.F.) and a Grant-in-Aid for Special Research in Subsidies for ordinary expenses of private schools from The Promotion and Mutual Aid Corporation for Private Schools of Japan (to K.K.).

### Conflict of Interest

None declared.

## References

1. Gemba, K., Fujimoto, N., Kato, K., Aoe, K., Takeshima, Y., Inai, K., and Kishimoto, T. (2012) National survey of malignant mesothelioma and asbestos exposure in Japan. *Cancer Sci.* **103**, 483–490
2. Robinson, B.W., Musk, A.W., and Lake, R.A. (2005) Malignant mesothelioma. *Lancet* **366**, 397–408
3. Carbone, M., Adusumilli, P.S., Alexander, H.R. Jr., Baas, P., Bardelli, F., Bononi, A., Bueno, R., Felley-Bosco, E., Galateau-Salle, F., Jablons, D., Mansfield, A.S., Minaai, M., de Perrot, M., Pesavento, P., Rusch, V., Severson, D.T., Taioli, E., Tsao, A., Woodard, G., Yang, H., Zauderer, M.G., and Pass, H.I. (2019) Mesothelioma: scientific clues for prevention, diagnosis, and therapy. *CA Cancer J. Clin.* **69**, 402–429
4. Nakano, T. (2008) Current therapies for malignant pleural mesothelioma. *Environ. Health Prev. Med.* **13**, 75–83
5. Muruganandan, S., Alfonso, H., Franklin, P., Shilkin, K., Segal, A., Olsen, N., Reid, A., de Klerk, N., Musk, A.B., and Brims, F. (2017) Comparison of outcomes following a cytological or histological diagnosis of malignant mesothelioma. *Br. J. Cancer* **116**, 703–708
6. Lv, J. and Li, P. (2019) Mesothelin as a biomarker for targeted therapy. *Biomark. Res.* **7**, 18
7. Sato, T., Suzuki, Y., Mori, T., Maeda, M., Abe, M., Hino, O., and Takahashi, K. (2014) Newly established ELISA for N-ERC/mesothelin improves diagnostic accuracy in patients with suspected pleural mesothelioma. *Cancer Med.* **3**, 1377–1384
8. Varki, A. (2017) Biological roles of glycans. *Glycobiology* **27**, 3–49
9. Pinho, S.S. and Reis, C.A. (2015) Glycosylation in cancer: mechanisms and clinical implications. *Nat. Rev. Cancer* **15**, 540–555
10. Kariya, Y., Kariya, Y., and Gu, J. (2017) Roles of Integrin alpha6beta4 glycosylation in cancer. *Cancers* **9**, 79
11. Liu, Y.C., Yen, H.Y., Chen, C.Y., Chen, C.H., Cheng, P.F., Juan, Y.H., Chen, C.H., Khoo, K.H., Yu, C.J., Yang, P.C., Hsu, T.L., and Wong, C.H. (2011) Sialylation and fucosylation of epidermal growth factor receptor suppress its dimerization and activation in lung cancer cells. *Proc. Natl. Acad. Sci. USA* **108**, 11332–11337
12. Seberger, P.J. and Chaney, W.G. (1999) Control of metastasis by Asn-linked, beta1-6 branched oligosaccharides in mouse mammary cancer cells. *Glycobiology* **9**, 235–241
13. van Putten, J.P.M. and Strijbis, K. (2017) Transmembrane mucins: signaling receptors at the intersection of inflammation and cancer. *J. Innate Immun.* **9**, 281–299
14. Buckhaults, P., Chen, L., Fregien, N., and Pierce, M. (1997) Transcriptional regulation of N-acetylglucosaminyltransferase V by the src oncogene. *J. Biol. Chem.* **272**, 19575–19581
15. Hatano, K., Miyamoto, Y., Nonomura, N., and Kaneda, Y. (2011) Expression of gangliosides, GD1a, and sialyl paragloboside is regulated by NF-kappaB-dependent transcriptional control of alpha2,3-sialyltransferase I, II, and VI in human castration-resistant prostate cancer cells. *Int. J. Cancer* **129**, 1838–1847
16. Kannagi, R., Yin, J., Miyazaki, K., and Izawa, M. (2008) Current relevance of incomplete synthesis and neo-synthesis for cancer-associated alteration of carbohydrate determinants–Hakomori's concepts revisited. *Biochim. Biophys. Acta* **1780**, 525–531
17. Pinho, S.S., Oliveira, P., Cabral, J., Carvalho, S., Huntsman, D., Gartner, F., Seruca, R., Reis, C.A., and Oliveira, C. (2012) Loss and recovery of Mgat3 and GnT-III mediated E-cadherin N-glycosylation is a mechanism involved in epithelial-mesenchymal-epithelial transitions. *PLoS One* **7**, e33191
18. Aryal, R.P., Ju, T., and Cummings, R.D. (2010) The endoplasmic reticulum chaperone Cosmc directly promotes in vitro folding of T-synthase. *J. Biol. Chem.* **285**, 2456–2462
19. Schietinger, A., Philip, M., Yoshida, B.A., Azadi, P., Liu, H., Meredith, S.C., and Schreiber, H. (2006) A mutant chaperone converts a wild-type protein into a tumor-specific antigen. *Science* **314**, 304–308
20. Kakugawa, Y., Wada, T., Yamaguchi, K., Yamanami, H., Ouchi, K., Sato, I., and Miyagi, T. (2002) Up-regulation of plasma membrane-associated ganglioside sialidase (Neu3) in human colon cancer and its involvement in apoptosis suppression. *Proc. Natl. Acad. Sci. USA* **99**, 10718–10723
21. Wagatsuma, T., Nagai-Okatani, C., Matsuda, A., Masugi, Y., Imaoka, M., Yamazaki, K., Sakamoto, M., and Kuno, A. (2020) Discovery of pancreatic ductal adenocarcinoma-related aberrant glycosylations: a multilateral approach of lectin microarray-based tissue glycomic profiling with public transcriptomic datasets. *Front. Oncol.* **10**, 338
22. Kuno, A., Kato, Y., Matsuda, A., Kaneko, M.K., Ito, H., Amano, K., Chiba, Y., Narimatsu, H., and Hirabayashi, J. (2009) Focused differential glycan analysis with the platform antibody-assisted lectin profiling for glycan-related biomarker verification. *Mol. Cell. Proteomics* **8**, 99–108
23. Takakura, D., Hashii, N., and Kawasaki, N. (2014) An improved in-gel digestion method for efficient identification of protein and glycosylation analysis of glycoproteins using guanidine hydrochloride. *Proteomics* **14**, 196–201
24. Kaji, H., Yamauchi, Y., Takahashi, N., and Isobe, T. (2006) Mass spectrometric identification of N-linked glycopeptides using lectin-mediated affinity capture and

glycosylation site-specific stable isotope tagging. *Nat. Protoc.* **1**, 3019–3027
25. Takakura, D., Harazono, A., Hashii, N., and Kawasaki, N. (2014) Selective glycopeptide profiling by acetone enrichment and LC/MS. *J. Proteomics* **101**, 17–30
26. Narasimhan, S. (1982) Control of glycoprotein synthesis. UDP-GlcNAc:glycopeptide beta 4-N-acetylglucosaminyltransferase III, an enzyme in hen oviduct which adds GlcNAc in beta 1-4 linkage to the beta-linked mannose of the trimannosyl core of N-glycosyl oligosaccharides. *J. Biol. Chem.* **257**, 10235–10242.
27. Irimura, T., Tsuji, T., Tagami, S., Yamamoto, K., and Osawa, T. (1981) Structure of a complex-type sugar chain of human glycophorin A. *Biochemistry* **20**, 560–566
28. Yamashita, K., Umetsu, K., Suzuki, T., Iwaki, Y., Endo, T., and Kobata, A. (1988) Carbohydrate binding specificity of immobilized Allomyrina dichotoma lectin II. *J. Biol. Chem.* **263**, 17482–17489
29. Gu, J., Nishikawa, A., Tsuruoka, N., Ohno, M., Yamaguchi, N., Kangawa, K., and Taniguchi, N. (1993) Purification and characterization of UDP-N-acetylglucosamine: alpha-6-D-mannoside beta 1-6N-acetylglucosaminyltransferase (N-acetylglucosaminyltransferase V) from a human lung cancer cell line. *J. Biochem.* **113**, 614–619
30. Koyota, S., Ikeda, Y., Miyagawa, S., Ihara, H., Koma, M., Honke, K., Shirakura, R., and Taniguchi, N. (2001) Down-regulation of the alpha-Gal epitope expression in N-glycans of swine endothelial cells by transfection with the N-acetylglucosaminyltransferase III gene. Modulation of the biosynthesis of terminal structures by a bisecting GlcNAc. *J. Biol. Chem.* **276**, 32867–32874.
31. Schachter, H. (1986) Biosynthetic controls that determine the branching and microheterogeneity of protein--bound oligosaccharides. *Biochem. Cell Biol.* **64**, 163–181
32. Schachter, H., Narasimhan, S., Gleeson, P., and Vella, G. (1983) Control of branching during the biosynthesis of asparagine-linked oligosaccharides. *Can. J. Biochem. Cell Biol.* **61**, 1049–1066
33. Abbott, K.L., Nairn, A.V., Hall, E.M., Horton, M.B., McDonald, J.F., Moremen, K.W., Dinulescu, D.M., and Pierce, M. (2008) Focused glycomic analysis of the N-linked glycan biosynthetic pathway in ovarian cancer. *Proteomics* **8**, 3210–3220
34. Nan, B.C., Shao, D.M., Chen, H.L., Huang, Y., Gu, J.X., Zhang, Y.B., and Wu, Z.G. (1998) Alteration of N-acetylglucosaminyltransferases in pancreatic carcinoma. *Glycoconj. J.* **15**, 1033–1037
35. Yoshimura, M., Nishikawa, A., Ihara, Y., Nishiura, T., Nakao, H., Kanayama, Y., Matuzawa, Y., and Taniguchi, N. (1995) High expression of UDP-N-acetylglucosamine: beta-D mannoside beta-1,4-N-acetylglucosaminyltransferase III (GnT-III) in chronic myelogenous leukemia in blast crisis. *Int. J. Cancer* **60**, 443–449
36. Yoshimura, M., Ihara, Y., Ohnishi, A., Ijuhin, N., Nishiura, T., Kanakura, Y., Matsuzawa, Y., and Taniguchi, N. (1996) Bisecting N-acetylglucosamine on K562 cells suppresses natural killer cytotoxicity and promotes spleen colonization. *Cancer Res.* **56**, 412–418
37. Iijima, J., Zhao, Y., Isaji, T., Kameyama, A., Nakaya, S., Wang, X., Ihara, H., Cheng, X., Nakagawa, T., Miyoshi, E., Kondo, A., Narimatsu, H., Taniguchi, N., and Gu, J. (2006) Cell-cell interaction-dependent regulation of N-acetylglucosaminyltransferase III and the bisected N-glycans in GE11 epithelial cells. Involvement of E-cadherin-mediated cell adhesion. *J. Biol. Chem.* **281**, 13038–13046.
38. Xu, Q., Isaji, T., Lu, Y., Gu, W., Kondo, M., Fukuda, T., Du, Y., and Gu, J. (2012) Roles of N-acetylglucosaminyltransferase III in epithelial-to-mesenchymal transition induced by transforming growth factor beta1 (TGF-beta1) in epithelial cell lines. *J. Biol. Chem.* **287**, 16563–16574
39. Yoshimura, M., Ihara, Y., Matsuzawa, Y., and Taniguchi, N. (1996) Aberrant glycosylation of E-cadherin enhances cell-cell binding to suppress metastasis. *J. Biol. Chem.* **271**, 13811–13815
40. Isaji, T., Gu, J., Nishiuchi, R., Zhao, Y., Takahashi, M., Miyoshi, E., Honke, K., Sekiguchi, K., and Taniguchi, N. (2004) Introduction of bisecting GlcNAc into integrin alpha5beta1 reduces ligand binding and down-regulates cell adhesion and cell migration. *J. Biol. Chem.* **279**, 19747–19754
41. Kariya, Y., Kato, R., Itoh, S., Fukuda, T., Shibukawa, Y., Sanzen, N., Sekiguchi, K., Wada, Y., Kawasaki, N., and Gu, J. (2008) N-Glycosylation of laminin-332 regulates its biological functions. A novel function of the bisecting GlcNAc. *J. Biol. Chem.* **283**, 33036–33045.
42. Kitada, T., Miyoshi, E., Noda, K., Higashiyama, S., Ihara, H., Matsuura, N., Hayashi, N., Kawata, S., Matsuzawa, Y., and Taniguchi, N. (2001) The addition of bisecting N-acetylglucosamine residues to E-cadherin down-regulates the tyrosine phosphorylation of beta--catenin. *J. Biol. Chem.* **276**, 475–480
43. Mendonsa, A.M., Na, T.Y., and Gumbiner, B.M. (2018) E-cadherin in contact inhibition and cancer. *Oncogene* **37**, 4769–4780
44. Pinho, S.S., Reis, C.A., Paredes, J., Magalhaes, A.M., Ferreira, A.C., Figueiredo, J., Xiaogang, W., Carneiro, F., Gartner, F., and Seruca, R. (2009) The role of N-acetylglucosaminyltransferase III and V in the post--transcriptional modifications of E-cadherin. *Hum. Mol. Genet.* **18**, 2599–2608
45. Rump, A., Morikawa, Y., Tanaka, M., Minami, S., Umesaki, N., Takeuchi, M., and Miyajima, A. (2004) Binding of ovarian cancer antigen CA125/MUC16 to mesothelin mediates cell adhesion. *J. Biol. Chem.* **279**, 9190–9198